RSC Advances

PAPER

View Article Online
View Journal | View Issue

Cite this: *RSC Adv.*, 2021, **11**, 14717

A nickel nanoparticle engineered $CoFe_2O_4/SiO_2$–NH_2@carboxamide composite as a novel scaffold for the oxidation of sulfides and oxidative coupling of thiols†

Mina Zohrevandi, Roya Mozafari and Mohammad Ghadermazi*

Received 28th February 2021
Accepted 4th April 2021

DOI: 10.1039/d1ra01592c

rsc.li/rsc-advances

The purpose of this work was to prepare a new Ni–carboxamide complex supported on $CoFe_2O_4$ nanoparticles ($CoFe_2O_4/SiO_2$–NH_2@carboxamide–Ni). The carboxamide host material unit generated cavities that stabilized the nickel nanoparticles effectively and prevented the aggregation and separation of these particles on the surface. This compound was appropriately characterized using FT-IR spectroscopy, FE-SEM, ICP-OES, EDX, XRD, TGA analysis, VSM, and X-ray atomic mapping. The catalytic oxidation of sulfides and oxidative coupling of thiols in the presence of the designed catalyst was explored as a highly selective catalyst using hydrogen peroxide (H_2O_2) as a green oxidant. The easy separation, simple workup, excellent stability of the nanocatalyst, short reaction times, non-explosive materials as well as appropriate yields of the products are some outstanding advantages of this protocol.

1. Introduction

In recent years, catalysts have attracted great attention due to their wide range of applications in different fields and has generated interesting discussions in chemistry.[1] Also, the design and preparation of green catalysts[2,3] have attracted much attention in academia and industries,[4–6] and hence, following green chemistry[7,8] is one of the important goals in synthetic organic chemistry.[9] Due to their application in human health hazards and environmental activities as well as economic importance, they have received exclusive attention.[10,11] To prepare heterogeneous catalysts, various supports have been proposed. The heterogenization of catalysts on solid supports is one of the appropriate methods to prevent wastage and can provide opportunities to recycle them from the reaction environment.[12–14] The use of these catalysts is a well-established method to control pollution. Thus, these catalysts have been extensively used in organic synthesis compared to homogenous catalysts because of economic and industrial aspects.[14,15] Supports for nanometer-sized catalysts have recently attracted great attention due to their appropriate surface area and outstanding chemical stability, and excellent activity in the liquid phase.[16,17] Functionalized nanoparticles are used as a feasible substitute for conventional materials as robust, active, and high surface area catalyst supports. Nevertheless, it is not possible to separate nanoparticles by conventional traditional methods such as filtration. Therefore, their separation from the reaction mixture requires special techniques, such as high-speed centrifugation,[18,19] which is not technologically and economically feasible.[20] Among these nanoparticles, superparamagnetic cobalt ferrite nanoparticles, due to their potential for catalyzing many organic reactions, have recently attracted much attention. These nanoparticles can be easily recovered from the reaction medium using an external magnetic field causing no need for filtration, and are reusable catalytic systems. In this regard, it is also reported that selecting the appropriate ligand groups is very important for strongly immobilization and robust metal linkages to nanoparticle cores.[21] However, the proper bonding allows us to have stable attachments of metals to magnetic nanoparticles, which makes it easy to recover the complex catalysts for further use in these procedures. Nanoscience has been enriched by the synthesis of new compounds that have different applications, such as carboxamide[22,23] derivatives that contain a ring junction nitrogen and suitable compounds are listed as ligand groups.[24,25] The conventional method for selective formation of carboxamides is by the reaction between an appropriate carboxylic acid and the corresponding amines in an organic solvent, for instance, pyridine. The synthesis of metal ions transitioning to organic ligands is of considerable interest due to the unique structural versatility and potential applications of various complexes containing amide groups that are structurally and magnetically interesting.[26–28] In this direction, a complex derived from carboxamide was considered as a coating material for nanoparticles and it has been used as an efficient and direct catalyst

Department of Chemistry, University of Kurdistan, P. O. Box 66135-416, Sanandaj, Iran. E-mail: mghadermazi@yahoo.com; Fax: +98 87 3324133; Tel: +98 87 33624133

† Electronic supplementary information (ESI) available. See DOI: 10.1039/d1ra01592c

in the synthesis of important products. The oxidation of sulfides to sulfoxides[29,30] due to their applications in fundamental researches is one of the particularly important transformations in organic compounds. Also, other extended usages consist of the synthesis of suitable chemicals and biological compounds, and as an intermediate for the production of various chemical and biological molecules, as well as antioxidants and stabilizers in engine and oil fuels. They have important medicinal properties such as anti-inflammatory and anti-cancer, and are also used in the treatment of diabetes and Alzheimer's; due to the basic applications of these compounds, they have received a lot of attention.[31] Although different methods have been developed for sulfide oxidation, catalytic oxidation switching to meet green chemistry has been established, but it remains challenging.[32–34] With the development of nanocatalysts for organic transformation, and carboxamide in the trapping and stabilizing of Ni nanoparticles, we present an efficient and reusable nanocatalyst for the oxidation of sulfides through the oxidative coupling of thiols with H_2O_2 as a green oxidant.

2. Experimental

2.1. Materials and methods

All materials were purchased from Sigma-Aldrich and Merck chemical and used without any further purification. The instruments used for the characterization of $CoFe_2O_4/SiO_2$–NH_2@carboxamide–Ni included SEM, EDX, XRD, VSM, FT-IR, TGA, and ICP-OES. The models of the apparatus are as following: the size distribution and the morphology of the nanocomposite were examined by using scanning electron microscopy (SEM) on an SEM TESCAN MIRA3 instrument. The elemental mapping and compositional analysis were performed using energy-dispersive X-ray spectroscopy (EDX) with a Keyex Delta Class I equipped with the SEM instrument. Powder X-ray diffraction (XRD) was performed on a Philips diffractometer of X'pert Company. Magnetic properties of fabricated nanocomposites were studied using a vibrating sample magnetometer (VSM) provided by the Meghnatis Daghigh Kavier Company. The FT-IR spectrum was obtained through the KBr disc method on a VERTEX 70 model BRUKER FT-IR spectrophotometer. The thermal stability of the nanocatalyst was studied by thermo-gravimetric analysis (TGA), which was performed on a Shimadzu DTG-60 instrument in the temperature range of 20–700 °C. The ICP-OES analyzer by PerkinElmer Optima 8300, was used for measuring the Ni loading and was a reliable solution for the elemental analysis of the catalyst. NMR spectra were recorded on a BRUKER Advance 400 MHz NMR spectrometer in $CDCl_3$ and DMSO.

2.2. Preparation of magnetic $CoFe_2O_4$ nanoparticles

First, Fe $(NO_3)_3 \cdot 9H_2O$ (3.23 g, 8.0 mmol), Co $(NO_3)_2 \cdot 6H_2O$ (1.2 g, 4.0 mmol) were dissolved in 30 mL distilled water at room

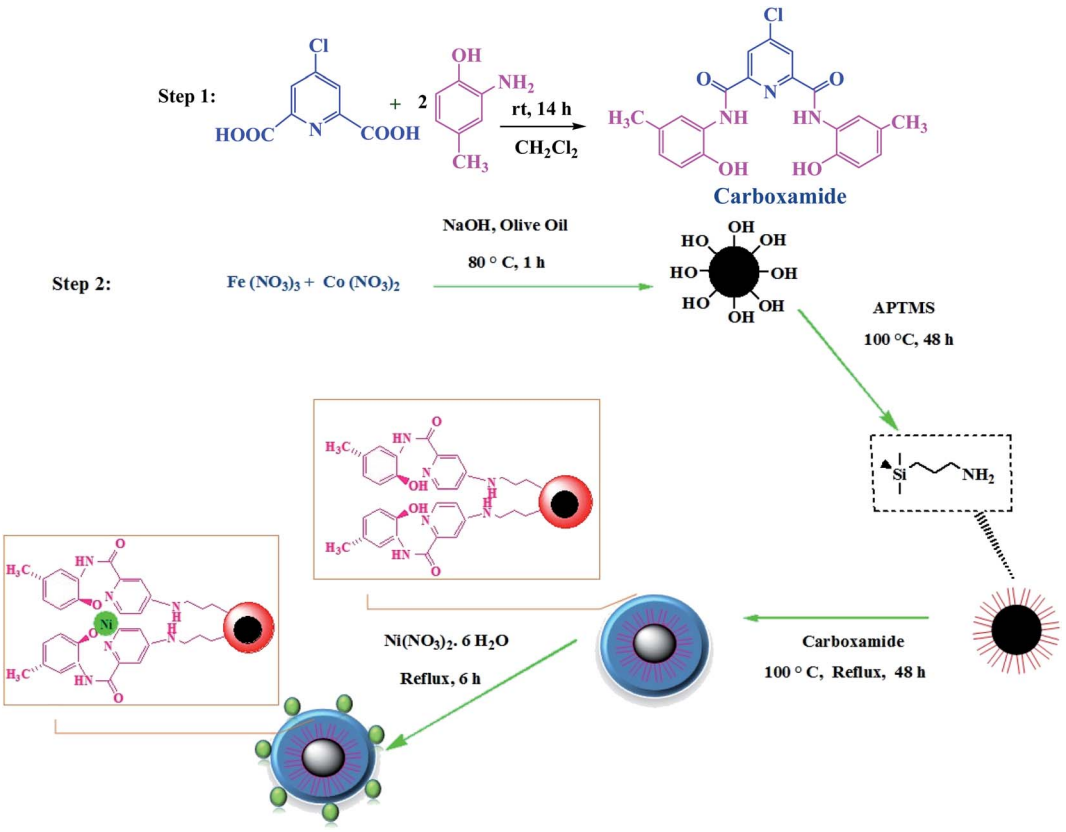

Scheme 1 The schematic pathway for preparing $CoFe_2O_4/SiO_2$–NH_2@carboxamide–Ni nanocomposite.

temperature. A solution of sodium hydroxide (10%) was added dropwise to the salt solution under constant stirring with a magnetic stirrer until the stabilization of pH to 11. Then, 0.3 mL of olive oil as a surfactant was added and heated at 80 °C for 1 h. After cooling the mixture, nano $CoFe_2O_4$ (dark precipitate) was separated by magnetic decantation and was washed several times with distilled water–ethanol mixture solution. The synthesized sample was dried at 60 °C for 12 h.

2.3. Preparation of 3-aminopropyl trimethoxysilane-coated $CoFe_2O_4$ ($CoFe_2O_4/SiO_2–NH_2$)

1 g of the prepared $CoFe_2O_4$ was well dispersed by ultrasonic vibration in anhydrous toluene (25 mL) for 15 min. Then, the linkage of 3-aminopropyl trimethoxysilane (APTMS) units was obtained on the support surface. APTMS (1 mL) was added slowly to the dispersion under vigorous stirring at reflux conditions for 48 h. The suspended substances were collected using a magnet and washed three times with ethanol/toluene to remove the remaining impurities and dried in a vacuum oven at 60 °C for 12 h. The resulting product was denoted as $CoFe_2O_4/SiO_2–NH_2$.

2.4. Preparation of carboxamide

Carboxamide was obtained according to the previously reported protocol.[35] In this method, 4-chloropyridine-2,6-dicarboxylic acid (0.183 g, 1 mmol) was dissolved in 20 mL of dry dichloromethane, then 2-amino-4-methyl phenol (0.246 g, 2 mmol) was added to it slowly by stirring occasionally, the resulting brown solution was stirred for 14 h at room temperature. The precipitated particles were formed and rinsed several times with $NaHCO_3$ (5%) to remove the remaining impurities. However, in this case, carboxamide was used as the organic ligand.

2.5. Preparation of the $CoFe_2O_4/SiO_2–NH_2$@carboxamide nanoparticles

In this step, the solution of $CoFe_2O_4/SiO_2–NH_2$ particles (1 g in 25 mL of distilled water), was prepared under constant stirring at 40 °C. At this time, carboxamide (0.6 g, 1.5 mmol) dissolved in chloroform (25 mL), was added to the combination mentioned above and the mixture solution was further stirred in a flask for 24 h under reflux. After cooling to room temperature, the generated solid was isolated using an external magnet, washed with water/ethanol, and dried at 60 °C for 24 h to afford a $CoFe_2O_4/SiO_2–NH_2$@carboxamide–Ni black solid.

2.6. Preparation of $CoFe_2O_4/SiO_2–NH_2$@carboxamide–Ni nanoparticles

In the final step, to prepare $CoFe_2O_4/SiO_2–NH_2$@carboxamide–Ni, (1 g) of the synthesized nanocomposite $CoFe_2O_4/SiO_2–NH_2$@carboxamide with $Ni(NO_3)_2·6H_2O$ (0.6 g 5.4 mmol) was mixed in ethanol (30 mL) under reflux condition at 80 °C for 6 h. Ultimately, the precipitates were isolated by using an external magnet. It was washed with ethanol three times and dried in a vacuum oven at 50 °C for 4 h. The resulting material was denoted as $CoFe_2O_4/SiO_2–NH_2$@carboxamide–Ni catalyst.

2.7. Procedure for the oxidation of sulfides to sulfoxides

For the synthesis of sulfoxide from the desired sulfide, in a 50 mL round bottom flask equipped with a magnetic stirrer, sulfide (1 mmol), H_2O_2 (0.5 mL) (33%), and $CoFe_2O_4/SiO_2–NH_2$@carboxamide–Ni catalyst (0.06 g) were added and the mixture was magnetically stirred at room temperature (25 °C). The reaction was checked using thin-layer chromatography (TLC), (using: hexane : ethyl acetate (4 : 1)).[36] Finally, after completing the reaction, the product was extracted from the reaction mixture with ethyl acetate. Then, the catalyst was separated using an external magnet, washed several times with ethanol, and dried in a vacuum oven at 80 °C for 5 h.

2.8. Procedure for the oxidation of thiol to disulfides

For the synthesis of disulfides, a mixture of thiol (1 mmol), and 0.4 mL H_2O_2 (33%) were stirred in the presence of $CoFe_2O_4/SiO_2–NH_2$@carboxamide–Ni catalyst (0.05 g) in ethanol (2 mL). The reaction was followed with TLC (using: hexane : ethyl acetate (4 : 1)). Finally, $CoFe_2O_4/SiO_2–NH_2$@carboxamide–Ni nanoparticles were magnetically separated and washed with ethanol several times. These particles were dried for 6 h in a vacuum oven at 70 °C. The structures of the products were recognized using their analytical and spectral (IR, ^1H, and ^{13}C NMR) data outlined in ESI.†

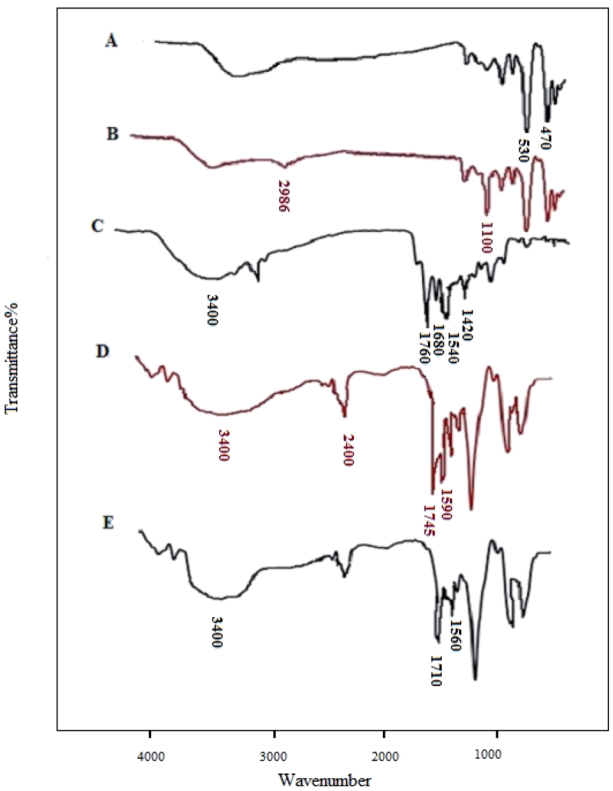

Fig. 1 FT-IR spectra of $CoFe_2O_4$ (A), $CoFe_2O_4/SiO_2–NH_2$ (B), carboxamide (C), $CoFe_2O_4/SiO_2–NH_2$@carboxamide (D), $CoFe_2O_4/SiO_2–NH_2$@carboxamide–Ni (E).

2.9. Selected spectral data

2.9.1. Methyl phenyl sulfoxide. ^{1}HNMR (400 MHz, DMSO, ppm): δ 4.16 (s, 4H), 7.713–7.732 (m, 10H); ^{13}CNMR (75 MHz, DMSO, ppm): δ 58.03, 129.6, 129.16, 128.81, 128.51, 127.5. IR (KBr) (cm^{-1}): ν (S=O): 1016–1072.

2.9.2. Benzyl phenyl sulfoxide. ^{1}HNMR (400 MHz, DMSO, ppm): δ 4.68 (s, 2H), 7.48–7.16 (m, 4H), 7.73–7.53 (m, 4H). ^{13}CNMR (75 MHz, DMSO, ppm): δ 61.15, 138.83–134.29, 1131.45, 130.9, 131.1, 129.0. IR (KBr) (cm^{-1}): ν (S=O): 1065.

2.9.3. 2,2′-Disulfanediyldiethanol. ^{1}HNMR (400 MHz, $CDCl_3$, ppm): δ 2.262–2.798 (m, 4H), 3.217 (m, 4H); ^{13}CNMR (100 MHz, $CDCl_3$, ppm): δ 41.43, 61.61. IR (KBr) (cm^{-1}): ν (S–S): 1058.

2.9.4. 1,2-Diphenyldisulfane. ^{1}HNMR (400 MHz, DMSO, ppm): δ 7.271–7.322 (m, 6H),7.325–7.382 (m, 4H); ^{13}CNMR (100 MHz, DMSO, ppm): δ 125.51, 127.28, 129.56, 136.83. IR (KBr) (cm^{-1}): ν (S–S): 1043.

2.10. Procedure for the recovery $CoFe_2O_4/SiO_2$–NH_2@carboxamide nanocatalyst

To recycle the catalyst in the sulfide oxidation reactions, the synthesized $CoFe_2O_4/SiO_2$–NH_2@carboxamide nanocomposite was separated as an efficient catalyst from the reaction mixture using an isolated external magnet and dried at 70 °C. The obtained nanocatalyst was used for the next reaction under optimal conditions. This procedure was repeated for eight runs, without significantly reducing on-target activity.

3. Results and discussions

The catalyst $CoFe_2O_4/SiO_2$–NH_2@carboxamide–Ni was prepared by the concise route shown in Scheme 1. To perform efficient immobilization of Ni on magnetic nanoparticles, initially, naked $CoFe_2O_4$ was linked with coated-APTMS containing NH_2 functional groups for better coordination. Subsequently, the carboxamide was synthesized *via* the reaction of 4-chloropyridine-2,6-dicarboxylic acid, and 2-amino-4-methyl phenol. Then, carboxamide supported on $CoFe_2O_4/SiO_2$–NH_2 ($CoFe_2O_4/SiO_2$–NH_2@carboxamide) was synthesized by a covalent linkage of Cl groups of the carboxamide with the amino (–NH) groups of APTMS. Finally, the catalyst was synthesized by the reaction of $CoFe_2O_4/SiO_2$–NH_2@carboxamide with $Ni(NO_3)_2$ through a stable exchange interaction between the nickel and carboxamide groups.

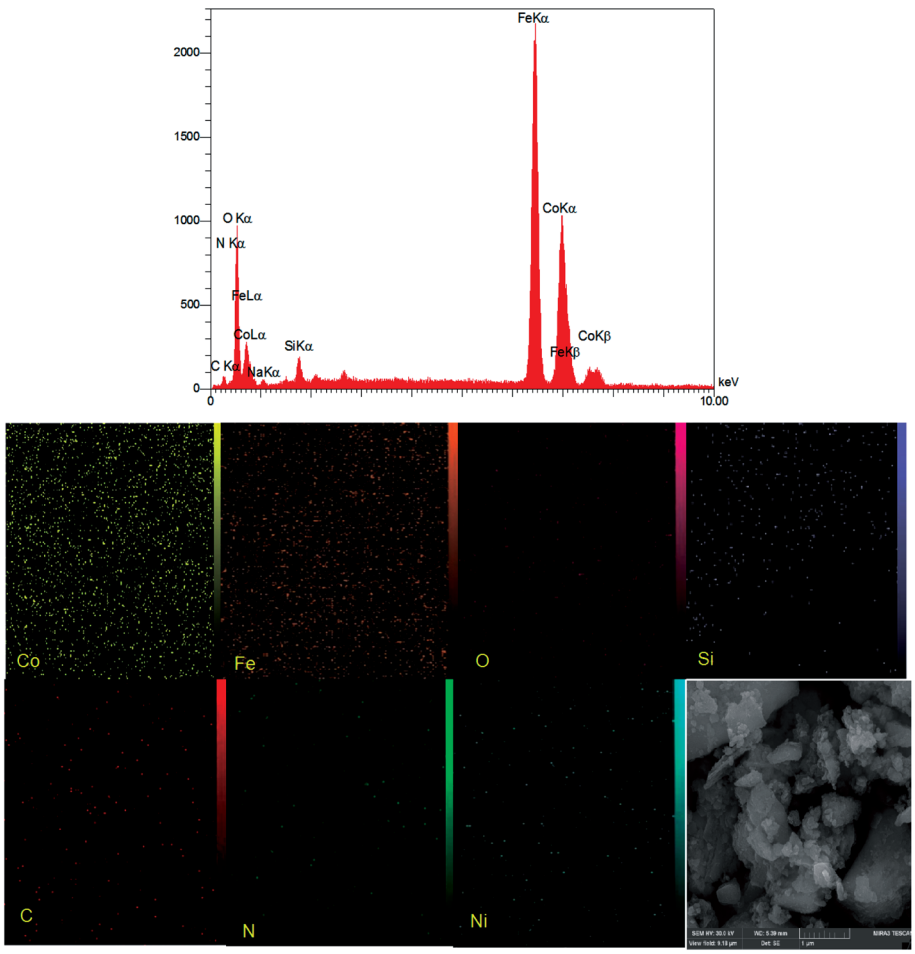

Fig. 2 EDX spectrum and elemental mapping of $CoFe_2O_4/SiO_2$–NH_2@carboxamide–Ni nanocomposite.

3.1. Catalyst characterization

The $CoFe_2O_4/SiO_2$–NH_2@carboxamide–Ni nanocomposite was successfully synthesized and the chemical properties and structure of the real catalyst were confirmed using XRD, FT-IR, SEM, EDX, ICP-OES, TGA, and VSM methods. The FT-IR spectra in the range of 400–4000 cm^{-1} of $CoFe_2O_4$, $CoFe_2O_4/SiO_2$–NH_2, carboxamide, $CoFe_2O_4/SiO_2$–NH_2@carboxamide, and $CoFe_2O_4/SiO_2$–NH_2@carboxamide–Ni nanocomposite are shown in Fig. 1. The presence of vibration bands at 470–530 cm^{-1} is assigned to the Fe–O bond in the $CoFe_2O_4$. The broad band at 3420 cm^{-1} can be related to the characteristic –OH bands of $CoFe_2O_4$ (Fig. 1A). The sharp peak at 1100 cm^{-1} and the peak at 3200 cm^{-1} are assigned to Si–O and NH_2 in $CoFe_2O_4/SiO_2$–NH_2, respectively (Fig. 1B). The stretching vibrations for the hydroxyl functional group (O–H) on the surface of carboxamide were recorded at 3000–3500 cm^{-1}, NH stretching band appeared at 3200 cm^{-1} in carboxamide and the peak at 1760 cm^{-1} was assigned to C=O stretching vibrations in carboxamide. Also, the stretching vibrations at 1680, 1540, and 1420 cm^{-1} in this compound are attributed to bonds in pyridine (Fig. 1C). The peak at about 1590 cm^{-1} and the peak at 1745 cm^{-1} are assigned to C–N vibrations and C=O stretching vibrations in $CoFe_2O_4/SiO_2$–NH_2@carboxamide–Ni, respectively (Fig. 1D), while for $CoFe_2O_4/SiO_2$–NH_2@carboxamide–Ni (Fig. 1E), this peak is shifted to 1710 cm^{-1} due to the coordination of the deprotonated oxygen and nitrogen carboxamide groups to the nickel.

The EDX elemental analysis was used to check the elemental composition in $CoFe_2O_4/SiO_2$–NH_2@carboxamide–Ni catalyst. The existence of elements Ni, Co, Fe, N, C, Si, and O in the catalyst confirmed the successful formation of $CoFe_2O_4/SiO_2$–NH_2@carboxamide–Ni catalyst (Fig. 2). Also, the images

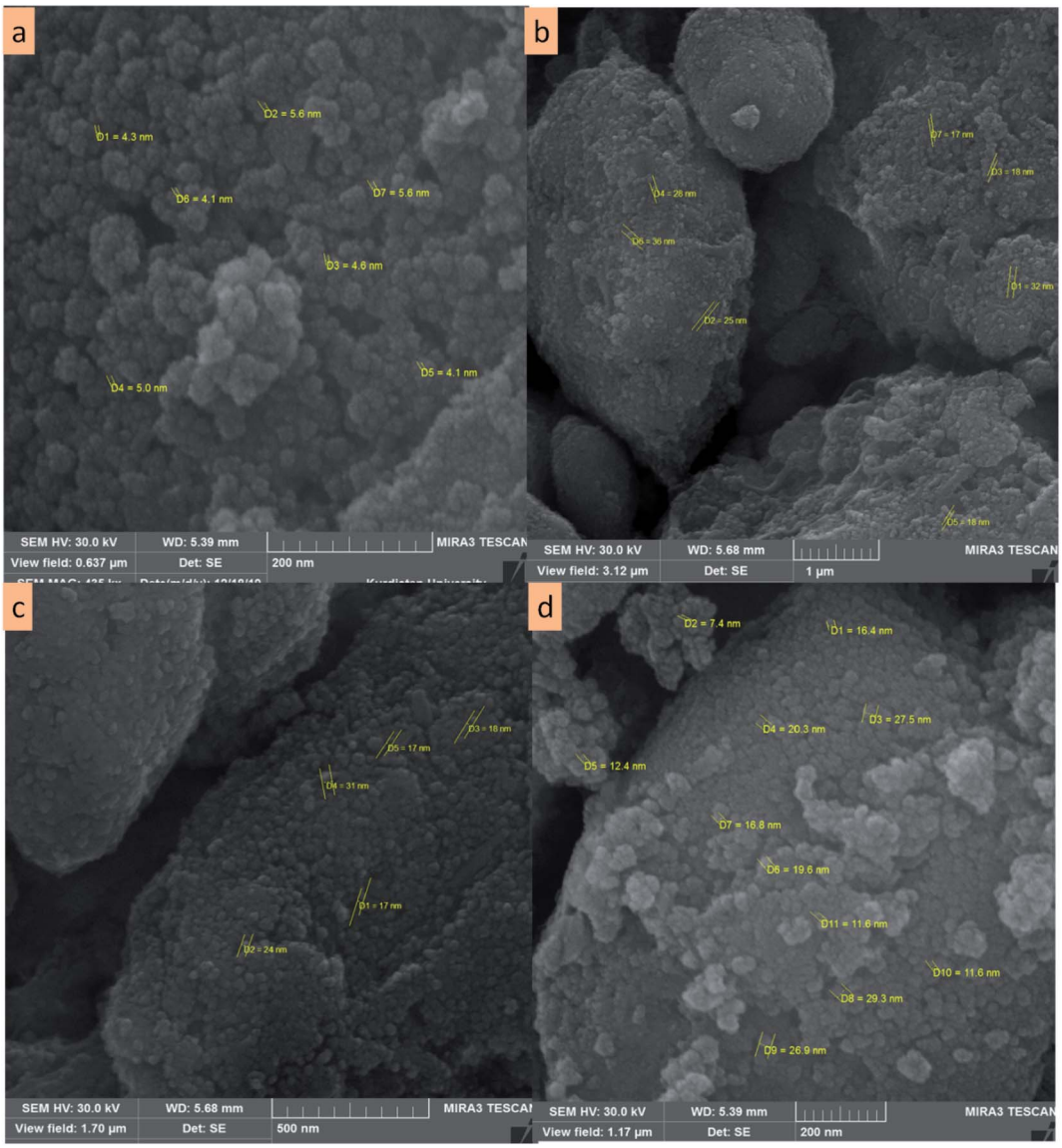

Fig. 3 FE-SEM images of $CoFe_2O_4$ (a) and $CoFe_2O_4/SiO_2$–NH_2@carboxamide–Ni nanocomposite at 1 µm (b), 500 nm (c), and 200 nm (d) magnifications.

obtained from the elemental mapping showed an uniform dispersion of Ni in the nanocomposite.

To identify the size and surface morphology, $CoFe_2O_4/SiO_2$–NH_2@carboxamide–Ni nanocomposite was studied using FE-SEM. As can be seen, spherical-shaped particles of $CoFe_2O_4$ have an average diameter of 4–5 nm (Fig. 3a) but the average diameter of $CoFe_2O_4/SiO_2$–NH_2@carboxamide–Ni changes from 10–30 nm to a bigger diameter, indicating modification and having a rather uniform coating of organic layers, and it can be concluded that $CoFe_2O_4/SiO_2$–NH_2@carboxamide–Ni particles were successfully synthesized (Fig. 3b–d).

Inductively definition ICP-OES analysis was used to determine the exact amount of nickel loaded on $CoFe_2O_4/SiO_2$–NH_2@carboxamide–Ni nanocomposite, and it was found to be 0.43 mmol g^{-1}.

The magnetic properties of $CoFe_2O_4$ and $CoFe_2O_4/SiO_2$–NH_2@carboxamide–Ni nanoparticles were measured using a vibrating sample magnetometer (VSM) at room temperature (Fig. 4). VSM measurements for the uncoated $CoFe_2O_4$ (Fig. 4a) and $CoFe_2O_4/SiO_2$–NH_2@carboxamide–Ni nanocomposite (Fig. 4b) showed that in the same field they were 68.7 and 27.3 emu g^{-1}, respectively. Also, a decrease in the magnetic properties of $CoFe_2O_4/SiO_2$–NH_2@carboxamide–Ni, compared to $CoFe_2O_4$ nanoparticles is due to the coating of $CoFe_2O_4$ nanoparticles by organic layers and a nickel complex.

Fig. 5 shows the thermo-gravimetric analysis (TGA) curve of the $CoFe_2O_4/SiO_2$–NH_2@carboxamide–Ni. The first weight loss (12.68%) between 50 and 250 °C corresponds to the removal of adsorbed water as well as the dehydration of the surface OH groups. The second significant weight loss (10.02%) from 260 to 360 °C is due to the decomposition of carboxamide complex residues. Some weight loss at around 370–530 °C is due to the disintegration of APTMS and carboxamide. In this way, the TGA curves also confirm the successful grafting of SiO_2–NH_2@-carboxamide–Ni onto the surface of $CoFe_2O_4$.

XRD patterns of $CoFe_2O_4$ and $CoFe_2O_4/SiO_2$–NH_2@-carboxamide–Ni catalyst are displayed in Fig. 6. The diffraction peaks for $CoFe_2O_4$ were observed at $2\theta = 21.17°$, 30.09°, 41.45°, 50.45°, 62.69°, 67.37°, and 74.45° that corresponded to (2 2 0), (2 2 2), (3 1 1), (4 0 0) (4 2 2), (5 1 1), (4 4 0) and (5 3 3) planes of the standard spinel structure of $CoFe_2O_4$ (JCPDS card no. 22-1086).[37] Also, no remarkable variation in the pattern of $CoFe_2O_4/SiO_2$–NH_2@carboxamide–Ni (Fig. 6b) catalyst suggested that it was retained after grafting of carboxamide on $CoFe_2O_4$ layers and the crystalline structure of $CoFe_2O_4$ (Fig. 6a) was not destroyed during the synthesis of the catalyst.

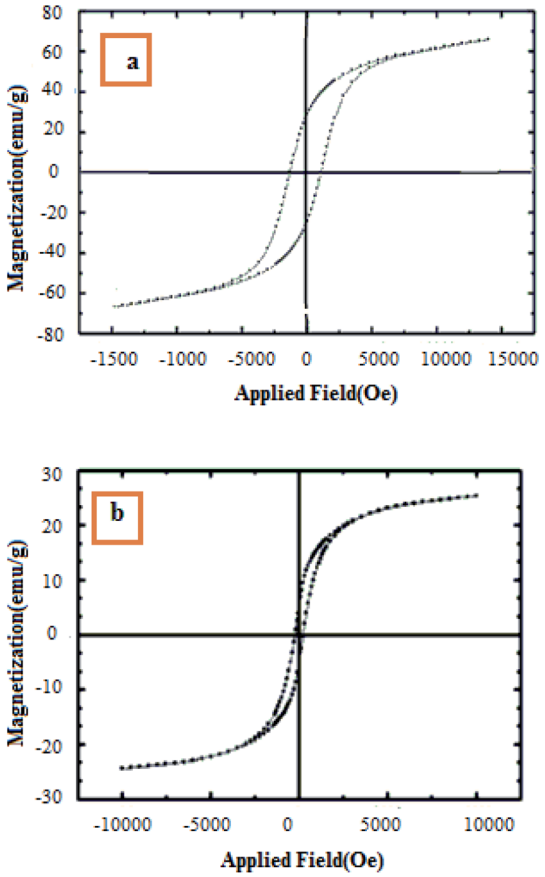

Fig. 4 VSM curves of $CoFe_2O_4$ (a), $CoFe_2O_4/SiO_2$–NH_2@-carboxamide–Ni nanocomposite (b).

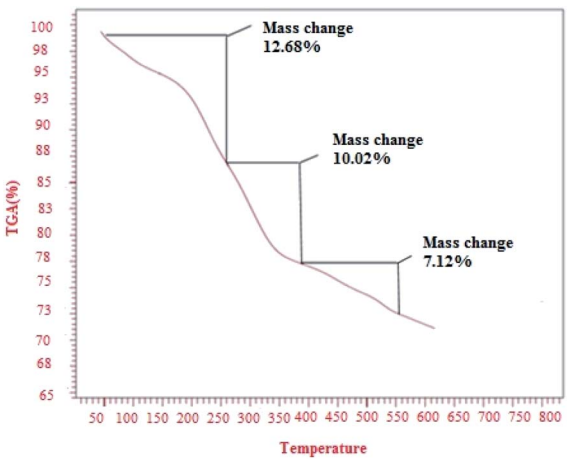

Fig. 5 The TGA curve of $CoFe_2O_4/SiO_2$–NH_2@carboxamide–Ni.

3.2. Catalytic activity

Due to the capability of $CoFe_2O_4/SiO_2$–NH_2@carboxamide–Ni as a mild and efficient catalyst, it was decided to use this synthesized catalyst for the oxidation of sulfides into corresponding sulfoxides (Scheme 2). Hence, methyl phenyl sulfide was investigated as a standard benchmark, and the influence of parameters such as the solvents, the amount of catalyst, H_2O_2, temperature, and oxidation agent's conditions were checked (Table 1). Initially, the effect of the catalyst amount on the reaction yield was studied. The amount of catalyst between 0.02–0.05 g on the reaction was examined for the reaction (Table 1, entries 6–9); the highest activity was observed in the presence of 0.04 g of the catalyst (Table 1, entry 12), and the oxidation reaction was also tested without a catalyst and the desired product was not obtained even after several hours (Table 1, entry 16). Then, the effects of the solvents on the model reaction

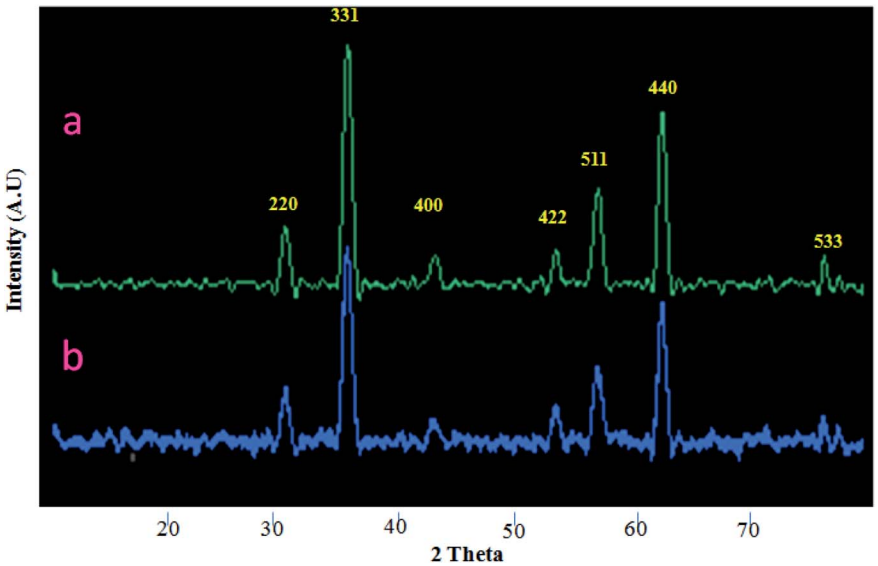

Fig. 6 The XRD patterns of $CoFe_2O_4$ (a), $CoFe_2O_4/SiO_2$–NH_2@carboxamide–Ni (b).

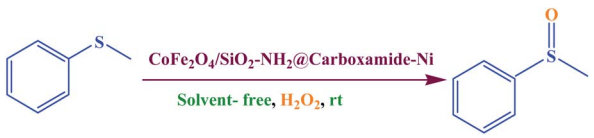

Scheme 2 General scheme for the oxidation of methyl phenyl sulfide.

were evaluated, the solvent-free conditions and a variety of solvents such as CH_3CN, EtOH, EtOAc, CH_2Cl_2, and H_2O were examined. Finally, it was found that solvent-free conditions gave the best results (Table 1, entry 12). The effect of temperature on the rate of the reaction was evaluated for the model reaction and, the best result was observed when the model reaction was performed at room temperature (Table 1, entry 12). Moreover, the table also shows that in case of the absence of H_2O_2, no reaction was performed (Table 1, entry 8), and considering the amount of H_2O_2 (Table 1, entries 6, 7, 12), increasing the amount of H_2O_2 proved to be the best choice for the reaction (Table 1, entry 12). Furthermore, the reaction was performed in the presence of $CoFe_2O_4/SiO_2$–NH_2@carboxamide and $CoFe_2O_4/SiO_2$–NH_2 catalysts, however, it did not proceed even after a long time. The obtained result shows the importance of the role of nickel nanoparticles in the catalytic activity for the synthesis of the product (Table 1, entries 17, 18).

After finding the results, however, to improve the reaction conditions, we employed various substituted sulfides for the

Table 1 Optimization of the oxidation of methyl phenyl sulfide by $CoFe_2O_4/SiO_2$–NH_2@carboxamide–Ni under different conditions[a]

Entry	Solvent (mL)	Catalyst (g)	H_2O_2 (mL)	Temperature (°C)	Time (min)	Yield (%)
1	CH_3CN	0.4	0.04	RT	8 h	45
2	EtOH	0.4	0.04	RT	6 h	52
3	EtOAc	0.4	0.04	RT	3 h	55
4	CH_2Cl_2	0.4	0.04	RT	2 h	68
5	H_2O	0.4	0.04	RT	140	70
6	Solvent-free	0.3	0.04	RT	100	78
7	Solvent-free	0.45	0.04	RT	50	94
8	Solvent-free	—	0.04	RT	2 h	40
9	Solvent-free	0.4	0.04	30	130	74
10	Solvent-free	0.4	0.04	40	130	70
11	Solvent-free	0.4	0.04	50	145	67
12	Solvent-free	0.4	0.04	RT	50	94
13	Solvent-free	0.4	0.05	RT	50	94
14	Solvent-free	0.4	0.03	RT	70	80
15	Solvent-free	0.4	0.02	RT	100	72
16	Solvent-free	0.4	—	RT	6 h	60
17	Solvent-free	0.4	$CoFe_2O_4/SiO_2$–NH_2@carboxamide	RT	5 h	68
18	Solvent-free	0.4	$CoFe_2O_4/SiO_2$–NH_2	RT	6 h	62

[a] Reaction conditions: methyl phenyl sulfide (1 mmol), H_2O_2 (0.4 mL), catalyst (0.04 g), and solvent-free.

synthesis of sulfoxides (Table 2). It is noteworthy that the reactions in the sulfoxide stage stop completely. For exploring the electronic effect on the performance, the range of *para*-substituted methyl phenyl sulfides was examined. The presence of the electron donor group increases the reaction process compared to that with the electron-withdrawing group, showing that the electronic nature of the sulfides affected the reaction rate (Table 2, entries 4 and 12). Furthermore, the oxidation of sulfides with sensitive functional groups such as hydroxyl did not affect functional groups, indicating high chemical selection.[38] (Table 2, entries 5, and 6). Interestingly, these systems can also be used in the oxidation from aliphatic sulfides, and good to excellent performance yields were obtained in the relevant sulfoxide systems (Table 2, entries 3, 8, and 10).

Table 2 Oxidation of various sulfides to sulfoxides in the presence of $CoFe_2O_4/SiO_2$–NH_2@carboxamide–Ni under optimization conditions[a]

Entry	Substrate	Time (min)	Yield (%)	Mp (°C)
1	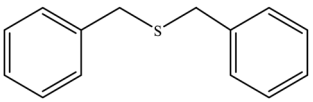	50	85	137–140 (ref. 39)
2	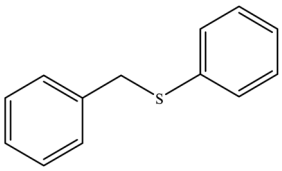	65	75	124–128 (ref. 40)
3	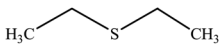	60	40	Oil[39]
4	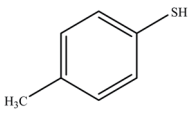	45	70	69–72 (ref. 41)
5	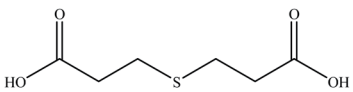	20	80	Oil[42]
6	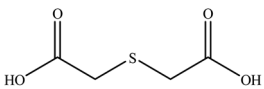	25	82	Oil[42]
7	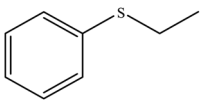	35	94	Oil[39]
8	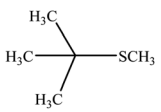	40	85	70–73 (ref. 42)
9	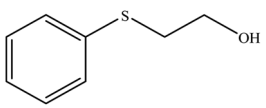	40	90	Oil[42]
10	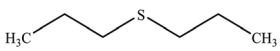	30	80	Oil[40]
11	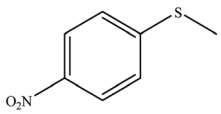	73	45	Oil[43]
12	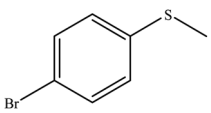	70	47	60–64 (ref. 43)

[a] Reaction conditions: sulfide (1 mmol), H_2O_2 (0.4 mL), catalyst (0.04 g), solvent-free, and room temperature conditions.

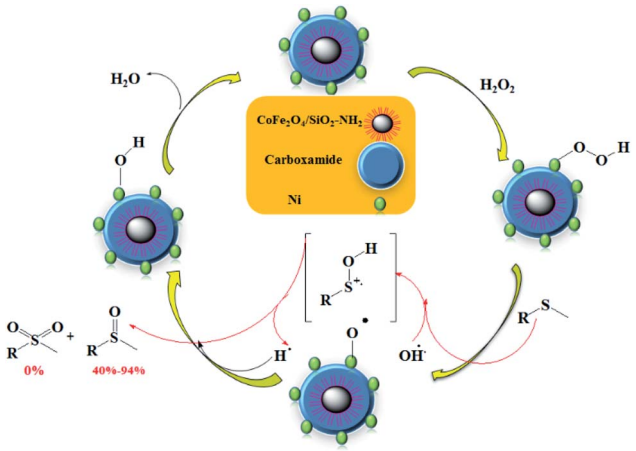

Scheme 3 $CoFe_2O_4/SiO_2$–NH_2@carboxamide–Ni catalyzed the oxidation of sulphide.

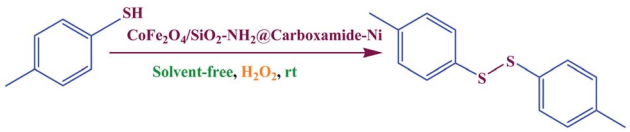

Scheme 4 General scheme for the oxidation of 4-methylbenzenethiol.

A possible explanation for the mechanism of sulfide using H_2O_2 as the oxidizing agent over $CoFe_2O_4/SiO_2$–NH_2@-carboxamide–Ni catalyst is proposed as shown in Scheme 3. Based on the literature report,[44] we propose that $CoFe_2O_4/SiO_2$–NH_2@carboxamide–Ni can easily react with H_2O_2 to form a Ni–OOH adduct. Then the Ni–OOH adduct may undergo cleavage of its O–OH bond to generate [Ni–O], and OH, radicals, where the compound can be subsequently oxidized to the corresponding sulfoxide by OH radicals. The reactivity can be linked to the topology of the Ni–OOH catalyst due to the relative ease of accessibility of the nucleophilic S atom on the sulfide to the Ni atom on the Ni–OOH active site. Sulfoxides are generated in good selectivity at 25 °C because the nucleophilic attack by sulfide is far superior to that of sulfoxide. Therefore, the present catalytic system utilizes cheap and readily available agents as a selective catalyst for clean oxidation of sulfide products and releases only innocuous water as the by-products.

Subsequently, we turned our attention to the oxidation reaction of thiols to disulfides, with H_2O_2 under different conditions. To optimize these reaction conditions and synthesis routes, we surveyed the synthesize of 4-methyl benzene thiol as the starting material under these different reaction conditions (Scheme 4). The test results are summarized in Table 3. Initially, the influence of the catalyst amount shows that the corresponding products were isolated in good to excellent yields with 0.03 g of $CoFe_2O_4/SiO_2$–NH_2@carboxamide–Ni as the most suitable amount (Table 3, entry 12). The reaction was performed without any catalyst, but it did not proceed for a long time (Table 3, entry 16). The effect of H_2O_2 as an oxidant on the oxidation of thiols was initially the reaction of the scientific model with 0.4 mL of H_2O_2 (33%), which was the most appropriate amount (Table 3, entry 12). Also, the reaction was tested in the absence of H_2O_2 and we found that the reaction did not progress well (Table 3, entry 8). The reaction was performed in different solvents in which the best result was obtained with solvent-free conditions (Table 3, entry 12). To investigate the effect of temperature on the reaction rate, this procedure was studied at various temperatures and the best one was at room temperature (Table 3, entry 12). More importantly, because of

Table 3 Optimization of the 4-methylbenzenethiol by $CoFe_2O_4/SiO_2$–NH_2@carboxamide–Ni under different conditions[a]

Entry	Solvent (mL)	Catalyst (g)	H_2O_2 (mL)	Temperature (°C)	Time (min)	Yield (%)
1	CH_3CN	0.4	0.03	RT	3 h	40
2	EtOH	0.4	0.03	RT	2 h	60
3	EtOAc	0.4	0.03	RT	1 h	52
4	CH_2Cl_2	0.4	0.03	RT	1 h	55
5	H_2O	0.4	0.03	RT	1 h	62
6	Solvent-free	0.3	0.03	RT	60	78
7	Solvent-free	0.45	0.03	RT	30	87
8	Solvent-free	—	0.03	RT	3 h	35
9	Solvent-free	0.4	0.04	RT	30	87
10	Solvent-free	0.4	0.02	RT	45	80
11	Solvent-free	0.4	0.01	RT	50	70
12	Solvent-free	0.4	0.03	RT	30	87
13	Solvent-free	0.4	0.03	30	40	73
14	Solvent-free	0.4	0.03	40	45	65
15	Solvent-free	0.4	0.03	50	55	60
16	Solvent-free	0.4	—	RT	5 h	60
17	Solvent-free	0.4	$CoFe_2O_4/SiO_2$–NH_2@carboxamide	RT	7 h	52
18	Solvent-free	0.4	$CoFe_2O_4/SiO_2$–NH_2	RT	7 h	38

[a] Reaction conditions: 4-methylbenzenethiol (1 mmol), H_2O_2 (0.4 mL), catalyst (0.03 g), and solvent-free.

Table 4 Oxidative 4-methylbenzenethiol by $CoFe_2O_4/SiO_2–NH_2$@carboxamide–Ni under optimization conditions[a]

Entry	Substrate	Time (min)	Yield (%)	Mp (°C)
1	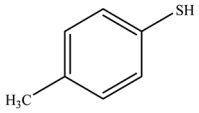	60	91	91–95 (ref. 41)
2	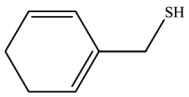	30	93	102–107 (ref. 45)
3	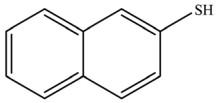	25	92	132–136 (ref. 40)
4	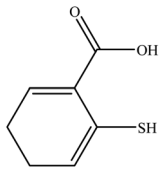	36	84	280–283 (ref. 46)
5	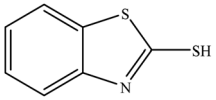	15	91	102–106 (ref. 46)
6	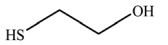	25	94	Oil[47]
7	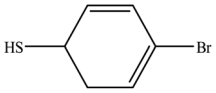	51	81	90–94 (ref. 40)
8	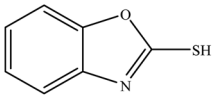	56	85	94–98 (ref. 46)
9	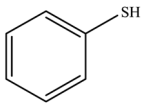	42	90	98–101 (ref. 48)
10	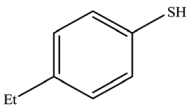	25	90	99–102 (ref. 40)
11	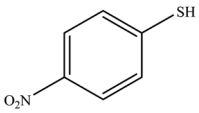	30	80	105–108 (ref. 40)

[a] Reaction conditions: sulfide (1 mmol), H_2O_2 (0.4 mL), catalyst (0.03 g), solvent-free, and room temperature conditions.

mild conditions of described heterogeneous systems, there is no overoxidation to sulfone for the oxidation of sulfides. Also, the reaction was performed in the presence of $CoFe_2O_4/SiO_2–NH_2$@carboxamide and $CoFe_2O_4/SiO_2–NH_2$ as the catalyst, but it did not proceed after a long time (Table 3, entries 17, 18).

Also, continuing with the optimal conditions, the oxidation reaction conditions of this protocol were tried with a wide range of different prepared thiol groups as shown in Table 4. After looking at the results, we found that, for the disulfide synthesis, the catalyst works well with good efficiency and with short reaction times. The electronic nature of the compounds affected the reaction rate. From a view of the electronic effect, the presence of the electron-donating group enhanced the reaction (Table 4, entry 11). Then, the study was performed on substrates containing electron-withdrawing groups (Table 4, entries 1, 10). We found that they need much more time than most electron-donating groups. Also, to further extend this method to the preparation of this catalytic system, aliphatic and aromatic sulfides were tested, and the acceptable yields of the corresponding disulfides were obtained.

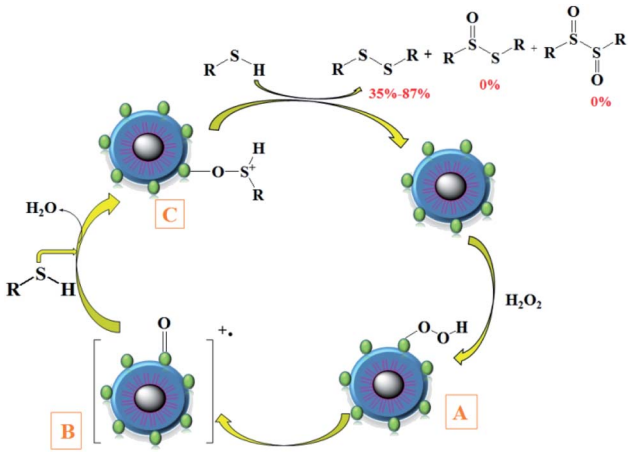

Scheme 5 $CoFe_2O_4/SiO_2$–NH_2@carboxamide–Ni catalyzed oxidative coupling of thiols to disulfides.

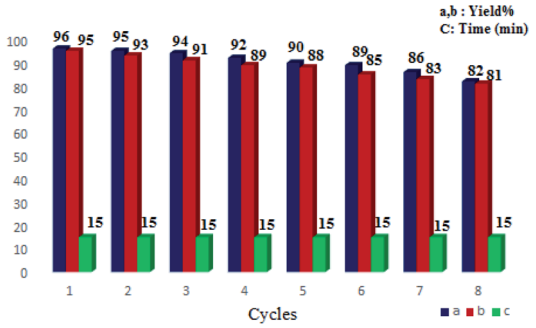

Fig. 7 Reusability of the $CoFe_2O_4/SiO_2$–NH_2@carboxamide–Ni for the oxidation of sulfides (a) and reusability of the $CoFe_2O_4/SiO_2$–NH_2@carboxamide–Ni for oxidation coupling reaction of thiols (b).

The proposed mechanism for the oxidation of thiols into disulfide in the presence of $CoFe_2O_4/SiO_2$–NH_2@carboxamide–Ni is shown in Scheme 5.[49,50] The reaction of H_2O_2 with Ni-catalyst leads to an intermediate A, which is converted to an active oxidant B. Next, the nucleophilic attack of the thiol on this intermediate gives cation C, which, in turn, produces the corresponding product.

In this study, $CoFe_2O_4/SiO_2$–NH_2@carboxamide–Ni was compared with the previously reported recoverable catalysts. As shown in Table 5, the oxidation reaction of sulfide (Table 5, entries 1–5) and thiol (Table 5, entries 6–11) is shown. This method is comparable to other reported catalysts in terms of reaction time, yield, and ease of catalyst separation in the presence of the synthesized catalyst.

3.3. Reusability of the $CoFe_2O_4/SiO_2$–NH_2@carboxamide–Ni

The reusability of $CoFe_2O_4/SiO_2$–NH_2@carboxamide–Ni for the oxidation of sulfides and the oxidation reaction of thiols was checked. The nanocomposite structure remained unchanged even after eight consecutive applications runs for the oxidation of sulfide and thiol (Fig. 7). To investigate changes in the chemical structure of the catalyst after the final cycle, FT-IR, TGA, and SEM analysis were performed and the results showed that the chemical structure of the catalyst was preserved without any change (Fig. 8).

3.4. ICP-OES technique

In the final investigation, the number of atoms loaded on the catalyst was measured using the ICP-OES technique. It was seen that Ni atoms in the fresh catalyst and recycled one after 8 times were 0.41 mol g^{-1} and 0.38 mol g^{-1} respectively, indicating that a minimum amount of Ni leaching happened in the catalytic process, confirming the stability and efficiency of the catalyst.

3.5. Hot filtration test

Also, the oxidation of sulfide in the presence of $CoFe_2O_4/SiO_2$–NH_2@carboxamide–Ni was investigated by hot filtration to determine whether the catalyst was heterogeneous or whether Ni was removed from the solid catalyst into the solution. In this experiment, under the optimized reaction conditions, we found product yield at 62% reaction half-time. The reaction was then repeated and during half of the reaction, the catalyst was removed from the reaction mixture by using a magnet. The reaction yield at this stage was 68%, which was heterogeneous

Table 5 Comparison of $CoFe_2O_4/SiO_2$–NH_2@carboxamide–Ni for the oxidation of methyl phenyl sulfide (entries 1–5) and 4-methylbenzenethiol (entries 6–11) with the previously reported catalysts

Entry	Substrate	Catalyst	Solvent	Time	Yield (%)	Ref.
1	Methyl phenyl sulfide	SBA-15/NH_2–FeQ_3	H_2O	3h	87	48
2	Methyl phenyl sulfide	Fe_3O_4@SiO_2–APTES–FeL	EtOH	2 h	99	51
3	Methyl phenyl sulfide	Fe_3O_4@SiO_2–APTES ($Fe(acac)_2$)	EtOH	2 h	92	52
4	Methyl phenyl sulfide	WOx/SBA-15(20)	TBHP	10 h	98	53
5	Methyl phenyl sulfide	$CoFe_2O_4$/Pr–NH_2 @carboxamide@Ni	Solvent-free	60	87	This work
6	4-Methylbenzenethiol	Fe_3O_4@tryptophan@Ni	Solvent-free	60	96	54
7	4-Methylbenzenethiol	Cu-SBTU@MCM-41	Solvent-free	40	97	55
8	4-Methylbenzenethiol	Fe_3O_4@tryptophan–Cu	EtOH	15	96	56
9	4-Methylbenzenethiol	Fe_3O_4–adenine–Ni	EtOH	70	97	57
10	4-Methylbenzenethiol	MCM-41@leucine–Ce(IV)	Solvent-free	40	97	58
11	4-Methylbenzenethiol	$CoFe_2O_4$/Pr–NH_2@carboxamide@Ni	Solvent-free	35	92	This work

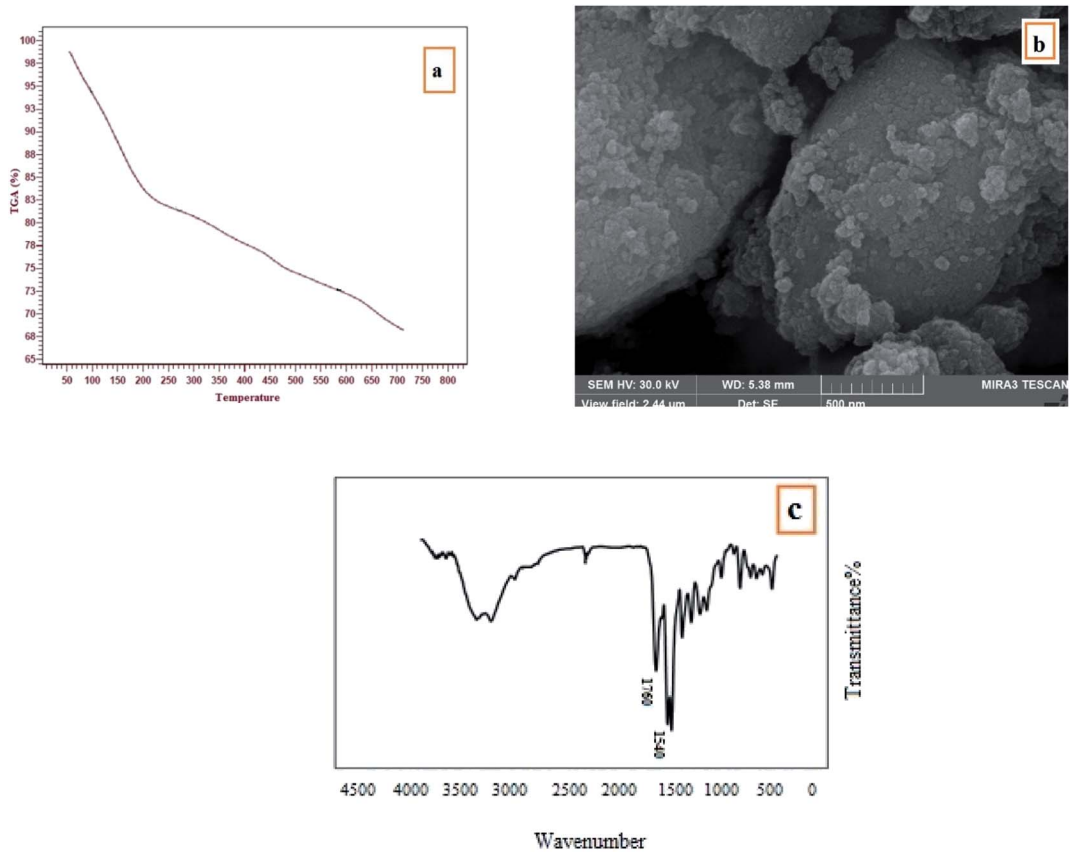

Fig. 8 TGA (a), SEM (b), and FT-IR (c) analyses of the reused $CoFe_2O_4/SiO_2–NH_2$@carboxamide–Ni after eight runs.

with a stable catalyst reaction and significant leakage of the effective nickel metal.

3.6. Catalyst poisoning test

Heterogeneity experiments were performed by the Hg poisoning study. In this way, Hg(0) can poison the catalyst, either by using a metal compound or by adsorption on the metal surface.[59] Sulfide oxidation was performed under the same conditions, except for the addition of Hg (1 mmol) to the reaction mixture at 50% conversion of methylphenyl sulfide to methylphenyl sulfoxide. Using this method, no product was obtained that is strong evidence of the heterogeneity of the nature of the catalyst.

4. Conclusions

We have described a simple strategy for the immobilization of a novel Ni–carboxamide complex on the modified surface of $CoFe_2O_4$ nanoparticles. $CoFe_2O_4/SiO_2–NH_2$@carboxamide–Ni was prepared by anchoring Ni on $CoFe_2O_4/SiO_2–NH_2$@-carboxamide. The activity of the catalyst was investigated in the oxidation of sulfides and the oxidative coupling of thiols at room temperature using H_2O_2 as a green oxidant. This method has several advantages, such as green conditions, high yield, short reaction times, efficient procedure, and low-cost separation and magnetic recyclability. Finally, the catalyst was separated using an external magnet and reused several times with no detectable changes in its catalytic efficiency. We anticipate that this protocol will be useful in the new research.

Conflicts of interest

There are no conflicts to declare.

Acknowledgements

The authors are grateful to the University of Kurdistan for sponsoring this research project.

Notes and references

1 V. I. Parvulescu and I. Fechete, *Catal. Today*, 2018, **306**, 1.
2 Y. Zhang, Y. Zhao and C. Xia, *Mol. Catal. A: Chem.*, 2009, **306**, 107–112.
3 P. Borah, X. Ma, K. T. Nguyen and Y. Zhao, *Chem. Int. Ed.*, 2012, **51**, 7756–7761.
4 M. Toda, A. Takagaki, M. Okamura, J. N. Kondo, S. Hayashi, K. Domen and M. Hara, Catalyst, *Nature*, 2005, **438**, 178.
5 H. Stachowiak, J. Kaźmierczak, K. Kuciński and G. Hreczycho, *Green Chem.*, 2018, **20**, 1–3.
6 T. Tamoradi, A. Ghorbani-Choghamarani, M. Ghadermazi and H. Veisi, *Solid State Sci.*, 2019, **91**, 96–107.

7 A. Michrowska, L. Gułajski, Z. Kaczmarska, K. Mennecke, A. Kirschningd and K. Grela, *Green Chem.*, 2006, **8**, 685–688.
8 T. Tamoradi, M. Ghadermazi and A. Ghorbani-Choghamarani, *Catal. Lett.*, 2018, **148**, 1834–1847.
9 (*a*) Y. Zhu, L. P. Stubbs, F. Ho, R. Liu, C. P. Ship, J. A. Maguire and N.S., *ChemCatChem.*, 2010, **2**, 365–374; (*b*) R. B. Nasir Baig and R. S. Varma, *Chem. Commun.*, 2013, **49**, 752–770.
10 S. Iravani, *Green Chem.*, 2011, **13**, 2638–2650.
11 R. Palaniswamy, R. Sandhya and S. Dhanyasri, *Int. J. Chemtech. Res.*, 2019, **12**, 292–298.
12 S. Hemmati, M. Hekmati, D. Salamat, M. Yousefi, B. Karmakar and H. Veisi, *Pre-proofs.*, 2019, **20**, 114359, DOI: 10.1016/j.poly.2020.114359.
13 Y. Zhu, L. P. Stubbs, F. Ho, R. Liu, C. P. Ship and J.A., *ChemCatChem.*, 2010, **2**, 365–374.
14 M. Ghadermazi, S. Moradi and R. Mozafari, *RSC Adv.*, 2020, **55**, 15052–15064.
15 T. Tamoradi, S. Taherabadi and M. Ghadermazi, *Polyhedron*, 2019, **171**, 305–311.
16 M. B. Gawande, P. S. Branco and R. S. Varma, *Chem. Soc. Rev.*, 2013, **42**, 3371–3393.
17 J. Xin, D. Lianna, L. Jessica, S. Bala, R. Shenqiang and V. C. Raghunath, *ACS Nano*, 2013, **7**, 1309–1316.
18 K. V. Ranganath, J. Kloesges, A. H. Schäfer and F. G. Angew, *Chem Int Ed*, 2010, **49**, 7786–7789.
19 T. Tamoradi, N. Moeini, M. Ghadermazi and A. Ghorbani-Choghamarani, *Polyhedron*, 2018, **153**, 104–109.
20 F. Shahbazi and K. Amani, *Catal. Commun.*, 2014, **55**, 57–64.
21 A. Skorobogaty and T. D. Smith, *Coord. Chem. Rev.*, 1984, **53**, 55–226.
22 J. F. Hartwig, *ACS Publications*, 2008, **41**, 1534–1544.
23 D. S. Surry and S. L. Buchwald, *Angew. Chem., Int. Ed.*, 2008, **47**, 6338–6361.
24 K. Ishihara and T. Yano, *Org. Lett.*, 2004, **6**, 1983–1986.
25 S. Meghdadi, M. Amirnasr, M. Zhiani, F. Jallili, M. Jari and M. Kiani, *Electrolysis*, 2017, **8**, 122–131.
26 M. Kiani, M. Bagherzadeh, S. Meghdadi, F. Fadaei-Tirani, M. Babaie and K. Schenk-Joß, *Inorg. Chim. Acta*, 2020, **506**, 119514, DOI: 10.1016/j.ica.2020.119514.
27 M. Lamac, J. Tauchman, I. Císařová and P. Štěpnička, *J. Am. Chem. Soc.*, 2011, **133**, 4240–4242.
28 M. Ito, T. Ootsuka, R. Watari, A. Shiibashi, A. Himizu and T. Ikariya, *J. Am. Chem. Soc.*, 2011, **133**, 4240–4242.
29 A. Shaabani and A. H. Rezayan, *Catal. Commun.*, 2007, **8**, 1112–1116.
30 L. Villalobos and T. Ren, *Chem. Commun.*, 2013, **28**, 52–54.
31 I. Fernández and N. Khiar, *Chem. Rev.*, 2003, **103**, 3651–3706.
32 N. Noori, M. Nikoorazm and A. Ghorbani-Choghamarani, *Phosphorus, Sulfur Silicon Relat. Elem.*, 2016, **191**, 1388–1395.
33 M. Azizi, A. Maleki, F. Hakimpoor, R. Ghalavand and A. Garavand, *Catal. Lett.*, 2017, **147**, 2173–2177.
34 A. Maleki and A. Sarvary, *RSC Adv.*, 2015, **75**, 60938–60955.
35 S. Mirfakhraei, M. Hekmati and H. Veisi, *Catal., Today*, 2017, 0920–5861, DOI: 10.1016/j.cattod.2017.06.002.
36 M. Kuriyama, R. Shimazawa and R. Shirai, *Composites, Part B*, 2019, **164**, 10–17.
37 M. Kooti and E. Nasiri, *J. Mol. Catal. A: Chem.*, 2015, **406**, 168–177.
38 M. Niakan, Z. Asadi and M. Masteri-Farahani, *J. Phys. Chem. Solids*, 2020, **147**, 109642, DOI: 10.1016/j.jpcs.2020.109642.
39 T. Tamoradi, M. Ghadermazi and A. Ghorbani-Choghamarani, *Catal. Lett.*, 2018, **148**, 857.
40 T. Tamoradi, M. Ghadermazi, A. Ghorbani-Choghamarani and S. Molaei, *Res. Chem. Intermed.*, 2018, **44**, 4259–4276.
41 U. Kurtan and A. Baykal, *Mater. Res. Bull.*, 2014, **60**, 79.
42 M. Niakan, Z. Asadi and M. Masteri-Farahani, *J. Phys. Chem. Solids*, 2020, 109642, DOI: 10.1016/j.jpcs.2020.109642.
43 T. Tamoradi, A. Ghorbani-Choghamarani and M. Ghadermazi, *New J. Chem.*, 2017, **41**, 11714–11721.
44 (*a*) Y. C. Fang, Q. Yan, Y. X. Jia and X. H. Duan, *New J. Chem.*, 2017, **41**, 2372; (*b*) S. Tanaka, Y. Kon, T. Nakashima and K. Sato, *RSC Adv.*, 2014, **4**, 37674; (*c*) S. Zhong, Y. Tan, Z. Fu, Q. Xie, F. Xie, X. Zhou, Z. Ye, G. Peng and D. Yin, *J. Catal.*, 2008, **154**, 256; (*d*) Y. Wang, Z. Fu, X. Wen, C. Rong, W. Wu, C. Zhang, J. Deng, B. Dai, S. R. Kirk and D. Yin, *J. Mol. Catal. A: Chem.*, 2014, **46**, 383–384; (*e*) Y. Wang, X. Wen, C. Rong, S. Tang, W. Wu, C. Zhang, Y. Liu and Z. Fu, *J. Mol. Catal. A: Chem.*, 2016, **103**, 411–418.
45 T. Tamoradi, A. Ghorbani-Choghamarani and M. Ghadermazi, *New J. Chem.*, 2017, **41**, 11714.
46 A. Ghorbani-Choghamarani, Z. Darvishnejad and M. Norouzi, *Appl. Organomet. Chem.*, 2015, **29**, 707.
47 M. Darabi, T. Tamoradi, M. Ghadermazi and A. Ghorbani-Choghamarani, *Transition Met. Chem.*, 2017, **41**, 703–710.
48 (*a*) N. Moeini, T. Tamoradi, M. Ghadermazi and A. Ghorbani-Choghamarani, *Appl. Organomet. Chem.*, 2018, **32**, e4445; (*b*) H. G. Hosseini and S. Rostamnia, *New J. Chem.*, 2018, **42**, 619–627.
49 R. Das and D. Chakraborty, *Tetrahedron Lett.*, 2010, **51**, 6255.
50 B. Karami1, M. Montazerozohori, M. Moghadam, M. H. Habibi and K. Niknam, *Turk. J. Chem.*, 2005, **29**, 539.
51 T. Karimpour, E. Safaei, B. Karimi and Y. Lee, *ChemCatChem*, 2018, **10**, 1889–1899.
52 A. Bayat, M. Shakourian-Fard, N. Ehyaei and M. Mahmoodi-Hashemi, *RSC Adv.*, 2014, **4**, 44274.
53 A. Bordoloi, A. Vinu and S. B. Halligudi, *Chem. Commun.*, 2007, **45**, 4806–4808.
54 N. Moeini, T. Tamoradi, M. Ghadermazi and A. Ghorbani-Choghamarani, *Appl. Organomet. Chem.*, 2018, **32**, 4445, DOI: 10.1002/aoc.4445.
55 A. Ghorbani-Choghamarani, B. Tahmasbi, P. Moradi and N. Havasi, *Appl. Organomet. Chem.*, 2016, **30**, 619–625.
56 N. Moeini, M. Ghadermazi and A. Ghorbani-Choghamarani, *Polyhedron*, 2019, **170**, 278–286.
57 T. Tamoradi, M. Ghadermazi and A. Ghorbani-Choghamarani, *Appl. Organomet. Chem.*, 2017, **32**, 3974, DOI: 10.1002/aoc.
58 H. Veisi, T. Tamoradi and B. Karmakar, *New J. Chem.*, 2019, **43**, 10343–10351.
59 A. Chatterjee and V. R. Jensen, *ACS Catal.*, 2017, **7**, 2543–2547.